Calculation of the resonance frequencies of the Rhodotron cavity using Green function.

J.M. Bassaler, CEA/DTA/LETI/DEIN, Centre d'Etudes de Saclay, 91191 Gif-sur-Yvette, France.
H. Baudrand, Groupe de Recherches en Micro-ondes, ENSEEIHT, 31069 Toulouse, France.

Abstract

We present a boundary integral method which allows to compute accurately the resonance frequencies of the Rhodotron accelerator modified coaxial cavity. Owing to this numerical method we can easily find out the geometry which optimizes the shunt impedance.

1. THE RHODOTRON ACCELERATOR

1.1 Use of a coaxial cavity

The whole characteristics of this new type of recirculating electron accelerator suitable for industrial applications are given in previous papers [1] [2]. The cavity is a $\lambda/2$ coaxial line short-circuited at both ends. Electrons are accelerated along diameters in the median plane where the electric field is radial and maximum and the magnetic field vanishes. The recirculation principle is shown on Figure 1.

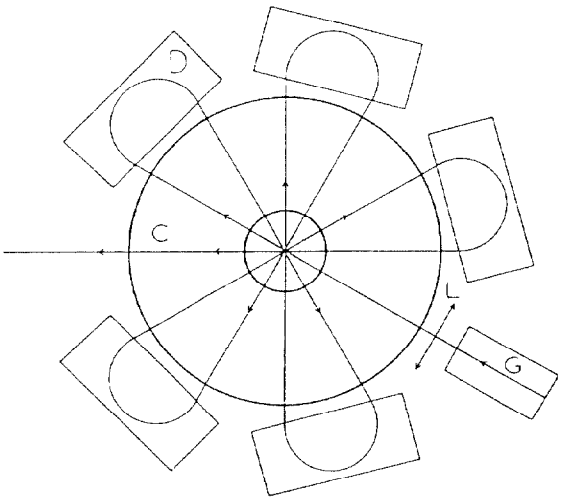

Figure 1: Median section of the accelerator and electron trajectory. D: Deflecting magnet C: Accelerating cavity L: Magnetic lens G: Electron gun

1.2 Shunt impedance improvement

Since in the fundamental resonance mode the magnetic field varies as 1/r and as a sinus maximum on the end faces, the main power losses are located at both ends of the inner conductor. We expect to reduce losses and thereby improve shunt impedance by opening this cylinder out as shown on Figure 2.

We use a boundary integral method to find out the eigen frequency and the shunt impedance of this modified coaxial cavity.

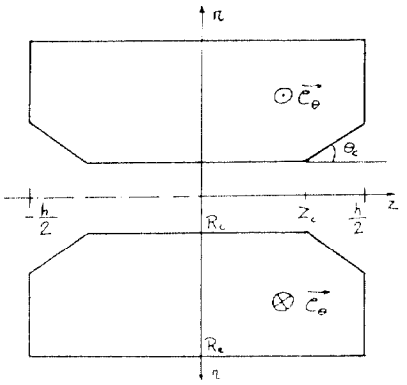

Figure 2: Longitudinal section of the modified cavity

2. BOUNDARY INTEGRAL METHOD

2.1 Background

The modified cavity is axisymmetric, hence the problem is reduced to two dimensions. As opposed to finite-element methods [3] where fields are calculated on many mesh points lying on a longitudinal section, all the unknown fields will be located on the path surrounding this surface. Using Green formula reduces the problem to a one-dimension equation.

2.2 Unknown function

As shown on Figure 3b an azimuthal magnetic field fulfils the boundary conditions even on the biased surface. On Figure 3a we see that the electric field can't be purely radial any longer. Hence the fundamental mode we are to find out is a Transverse Magnetic mode with axial symmetry; E_θ, H_r and H_z vanish. We can express the electric field components with the derivatives of the magnetic field $H = H_\theta(r,z)$ which we will take as unknown function:

$$E_r = \frac{j}{\omega \varepsilon_0} \frac{\partial H_\theta}{\partial z} \qquad E_z = -\frac{j}{\omega \varepsilon_0} \frac{\partial}{\partial r}(r H_\theta) \tag{1}$$

The equation it must fulfil is:

$$\mathcal{L}(H_\theta) = \Delta H_\theta - \frac{H_\theta}{r^2} + k_0^2 H_\theta =$$

$$\left(\frac{\partial^2}{\partial z^2} + \frac{\partial^2}{\partial r^2} + \frac{1}{r}\frac{\partial}{\partial r} + k_0^2 - \frac{1}{r^2} \right) H_\theta = 0 \tag{2}$$

Boundary conditions must be satisfied on path C (see Figure 4):

$$\frac{\partial H_\theta}{\partial n} = \vec{n} \cdot \overrightarrow{\text{grad}}\, H_\theta = 0 \tag{3}$$

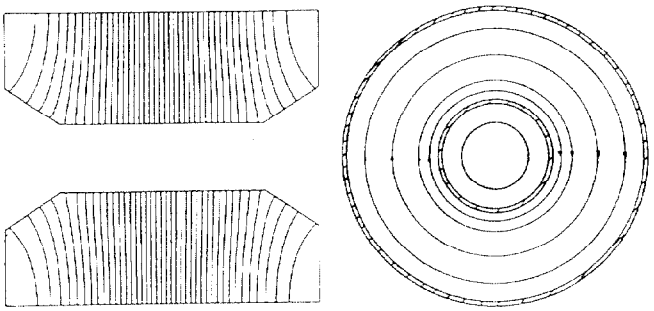

Figure 3: a) Electric field lines b) Magnetic field lines

2.3 Use of Green identity

Green function associated to the operator is defined by:

$$\mathcal{L}(G(r,z)) = \delta(r-r_0) \cdot \delta(z-z_0) \tag{4}$$

Let us use Green identity

$$\iint_{\mathcal{S}} (H \Delta G - G \Delta H)\, dS = \int_{\mathcal{C}} (H\, \overrightarrow{\text{grad}} G - G\, \overrightarrow{\text{grad}} H).\vec{n}\, dl \tag{5}$$

Instead of taking free space Green function [4] we add the following boundary condition on the path C' bounding the initial cavity (dashes on Figure 4).

$$\vec{n}.\overrightarrow{\text{grad}} G = 0 \tag{6}$$

The field can be expressed at any point of the surface or the boundary as a function of the field lying on the biased segments only [4]

$$C(r,z).H(r,z) = -\int_{ABUCD} H(r_0,z_0)\, \overrightarrow{\text{grad}}\, G(r,z,r_0,z_0).\vec{n}\; r_0 dl_0 \tag{7}$$

where C(r,z) = 1 on the surface and 1/2 on the boundary

2.4 Green function

It may be expanded as a linear combination of TEM and TM modes of the coaxial cavity:

$$G(r,z,r_0,z_0) =$$

$$\frac{2}{h} \sum_{n=0}^{\infty} \sum_{p=0}^{\infty} \frac{\xi(p)}{\mathcal{B}_n^2\, \Delta k_{np}^2} B_n(r) B_n(r_0) \cos\left(\frac{p\pi}{h}(z+\frac{h}{2})\right) \cos\left(\frac{p\pi}{h}(z_0+\frac{h}{2})\right)$$

$$(n,p) \neq (0,0)$$

$$\mathcal{B}_n^2 = \int_{R_i}^{R_e} \mathcal{B}_n^2(r) r\, dr \qquad \Delta k_{np}^2 = k_0^2 - k_{cn}^2 - \left(\frac{p\pi}{h}\right)^2$$

$$\xi(0) = \frac{1}{2} \quad \xi(p\neq 0) = 1 \text{ and } \mathcal{B}_0(r) = \frac{1}{r},\ k_{c0} = 0$$

$$\mathcal{B}_n(r) = A_n J_1(k_{cn} r) + B_n Y_1(k_{cn} r) \tag{8}$$

A_n, B_n, and k_{cn} are set by boundary conditions [5]. We use a projection to find out the coefficients in the double sum.

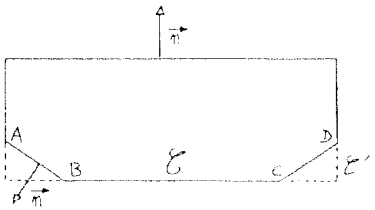

Figure 4: Integration paths

2.5 Eigenvalue equation

Searching separately symmetric and antisymmetric modes allows to reduce the unknown function domain to CD. To operate computation we divide this segment into Ns subsegments on which H is assumed to be constant. Replacing Green function (8) into Equation (7) yields:

$$H(r_i,z_i) = \sum_{n=0}^{\infty} \sum_{p\ (p \text{ even or odd})} \mathcal{P}_{np}\, B_n(r_i) \cos\left(\frac{p\pi}{h}(z_i+\frac{h}{2})\right)$$

$$\mathcal{P}_{np} = -\frac{8}{h}\xi(p) \frac{\delta}{\mathcal{B}_n^2\, \Delta k_{np}^2} \sum_{j=1}^{N_S} \left[k_{cn} B_n^0(r_j) \cos\left(\frac{p\pi}{h}(z_j+\frac{h}{2})\right) \cos\theta_c \right.$$

$$\left. + \frac{p\pi}{h} B_n(r_j) \sin\left(\frac{p\pi}{h}(z_j+\frac{h}{2})\right) \sin\theta_c \right] H(r_j,z_j) r_j \tag{9}$$

The field on each image point (r_i,z_i) located on CD is related to the field on every source point (r_j,z_j) located on the same segment. The set of point-matching equations can be expressed in the following vector form:

$$\left(H_i \right) = \left(A_{ij} \right)\left(H_j \right) \tag{10}$$

The frequencies which cancel the determinant Det (I-A) correspond to resonances.

3. RESULTS

3.1 Comparison with finite-element calculus and experiment

We compared the results provided by our code with those given by the finite-element code SUPERFISH [3] and with the measures performed on our prototype (Ri = 0.1125 m, Re = 0.45 m, h = 0.916 m, Zc = 0.298 m, θc = 34.4°, f = 178.9 Mhz).

We varied the number of subsegments Ns and the number of modes (Nmax.Nmax) in Green function expression, and found out a frequency that we compared with the accurate value provided by SUPERFISH; the error is plotted on Figure 5. We can notice a fast convergence: (Ns = 20, Nmax = 30) yields a precision better than 0.1%. It should be noted that the matrix size is Ns^2.

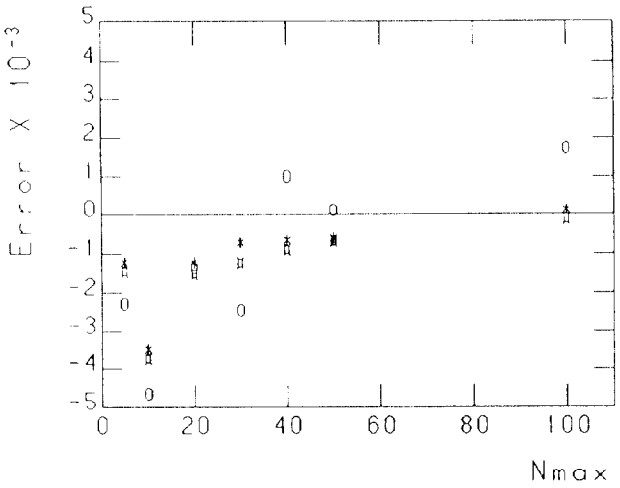

Figure 5: Accuracy versus number of modes and segments
O Ns = 5 □ Ns = 10 ✻ Ns = 20

When evaluating quality factor and shunt impedance the error is only a few percent. (Q = 36000, Zsh = 14.9 MΩ for a copper cavity)

We also predict with a good accuracy higher-order mode frequencies as shown on Table 1

3.2 Memory space and computing time

In SUPERFISH [6], if the surface is described by N^2 mesh points the involved memory space is proportional to N^3 whereas computing time varies as N^4.

In our code, if there are N subsegments and Nm^2 modes, the matrix size is N^2 only, whereas computing time varies as $N^2 . Nm^2$

3.3 Shunt impedance optimization

The main feature of our code is the capability of defining the frequency as a parameter and geometric dimensions as variables. Hence geometric dimensions corresponding to a fixed frequency can be found out very easily since they cancel the determinant. When varying these dimensions we could find a smooth maximum of shunt impedance (10% improvement) around the values Zc = 0.32 m and θc = 35°.

Mode	Sfish	Green	Meas.
TEM1	178.9	178.8	178.9
TEM2	344.2	343.7	343.8
TEM3	544.2	543.7	544.0
TM010	450.9	451.2	450.1
TM011	465.3	465.2	463.8
TM012	579.8	580.3	

Table 1: Fundamental and higher-order mode frequencies given by Superfish, our method and measurements

CONCLUSION

This boundary integral method provides accurate results within a small memory space. It can easily be turned out into a tool for calculation of modified coaxial cavity dimensions, in order to optimize shunt impedance.

REFERENCES

[1] J. Pottier, "A new type of RF electron accelerator: the Rhodotron", Nucl. Instr. Meth. Phys. Res., Vol B40/41, pp 943-945, 1989

[2] A. Nguyen et al., "Rhodotron first operations", proc. 2nd European Particle Accelerator Conference, Vol 2, Nice, France, 1990, pp 1840-1841

[3] K.Halbach, R.F. Holsinger, "Superfish, a computer program for evaluation of RF cavities with cylindrical symmetry", Particle Accelerators, Vol 7, pp 213-222, 1976

[4] M. Tuschimoto et al., "Boundary element analysis of axisymmetric resonant cavities", IEEE Trans. on Magnetics, Vol 24, pp 2500-2502, November 1988